arrhythmogenic, and removal of the left stellate ganglion has anti-arrhythmic effects. However, detailed studies into differential sympathetic innervations and effects on regional cardiac electrophysiology are lacking.

Purpose: This study will investigate the regional heterogeneities in ventricular electrophysiological parameters and the differential effects of the left and right sympathetic neurones.

Methods: Using the isolated innervated rabbit heart preparation, optical action potentials were obtained with the voltage sensitive dye di-4-ANEPPS over the anterior left ventricle using a Hamamatsu 16 × 16 element photodiode array. (n=12). The spinal cord was stimulated with both sympathetic chains intact (Bilateral sympathetic stimulation; SS), after removal of the left sympathetic chain (left denervation; LD) and after both chains were removed (left and right denervation; LRD). Heart rate, action potential duration (APD), action potential duration restitution (RT), dispersion of repolarisation (DOR) and effective refractory period (ERP) were measured. Data are Mean±SEM; compared using ANOVA or paired t-test.

Results: SS increased heart rate from 130.9±7.2 bpm to 216±3.9 bpm (P<0.0001, 74.5±10.5% increase). Spinal stimulation after LD still produced a large heart rate increase from 127.5± 5.5 bpm to 170±7.1 bpm (P<0.0001, 39.2±8.2%). After LRD, stimulation produced no change in heart rate. SS caused shortening of APD across the ventricle (mean APD: 148.2±1.2 ms) when compared to baseline (154.4±1.5 ms), with the greatest shortening observed at the base and free-wall. After LD, stimulation caused much less shortening (154.7±1.2ms) from baseline (157.3±1.4ms). There was no change in APD during stimulation after LRD. The maximum slope of RT displayed the same trend as APD as the increase in slope values observed during SS was greatly reduced after LD and eliminated after LRD. DOR increased from 4.1±0.3 to 5.2±0.4 with SS (P>0.05), from 6.2±0.8 to 6.4±0.8 after LD (P=NS) and there was no change after LRD. ERP decreased from 171.7±2.4 ms to 157.8±2.2 ms with SS (P<0.0001, -8.1±1.3%) and there was less of a decrease from 171.1±2.2 ms to 169.4±1.9 ms after LD (P<0.0001, -2.3±1.0%). There was no change in ERP from baseline after LRD.

Conclusion: This study highlights preferential electrophysiological effects at the base of the ventricle from stimulating left sympathetic neurones, and improves the understanding of the mechanisms behind the dominant influence of the left sympathetic neurones on cardiac excitability and arrhythmic mechanisms. These results have implications in refining treatment modalities involving sympathetic innervation such as stellectomy.

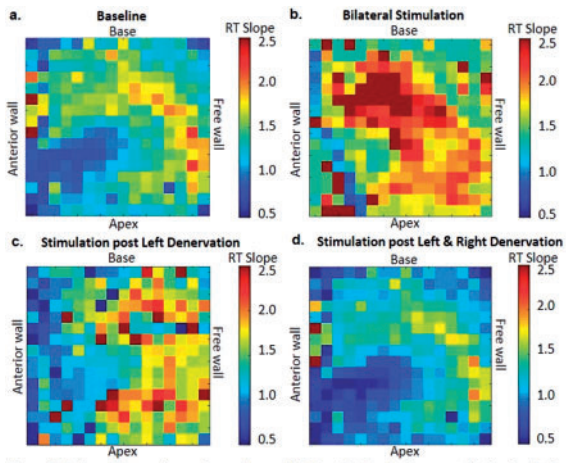

Figure 1. Regional changes in maximum slope of APD restitution during sympathetic stimulation and removal of sympathetic chains

Abstract P134 Figure.

P135

Role of cytokines of the TGF beta family in the atrial structural remodelling underlying atrial fibrillation in aortic stenosis patients

V. Exposito Garcia[1]; R. Garcia Lopez[2]; MA. Hurle Gonzalez[2]; JF. Nistal Herrera[1]
[1]University Hospital Marques de Valdecilla, Santander, Spain; [2]University of Cantabria, Santander, Spain

Funding Acknowledgements: Founding: FIS PI15/01224, Maratón TV3 FLM16/20.

Background: Studies on patients and animal models suggest the importance of atrial structural remodelling and fibrosis in the development of atrial fibrillation (AF). The auto-paracrine action of transforming growth factor-βs (TGFβs) on myocardial cells has been suggested to play a role in this process. The TGFβ superfamily of cytokines is composed, among others, of the profibrotic TGFβ and anti-fibrotic bone morphogenetic protein-7 (BMP-7). The role of micro-RNAs (miR) regulated by the TGFβ family in cardiac pathologies, including fibrosis, has been recently recognized.

Purpose: To demonstrate that AF under pressure overload is associated with atrial wall disequilibrium in TGFβ-1/BMP-7-mediated signalling and fibrosis-regulatory miRNAs.

Methods: Patients with aortic stenosis (AS) and AF (n=23) were matched with patients on sinus rhythm (n=23) according to age, gender and left ventricular ejection fraction. Right atrium biopsies were analysed by qPCR and in situ hybridization.

A cohort of patients who underwent cardiac surgery because of non-pressure overload cardiopathies was selected to validate the specificty of our findings.

Results: TGF-ß1, COL1A1, COL3A1, FN-1 and lysyl oxidase (LOX) were up-regulated in right atrial wall of AF patients with AS. TGF-β1 positively correlated with COL1A1, COL3A1, FN-1 and LOX. On the other hand, BMP-7 mRNA expression was down-regulated. miR-1, miR-133a, miR-133b and miR-29 expressions were significantly reduced. These changes were not observed in AF patients with non-pressure overload cardiopathies.

Conclusions: The unbalance between pro-fibrotic TGFβ1and anti-fibrotic BMP-7 facilitates pathological structural remodelling and AF development in AS patients. The increased pro-fibrotic transcriptional activity due to up-regulation of TGFβ1 expression was related to down-regulation of anti-fibrotic miRNAs (miR-1, miR-133 and miR-29).

P136

Defective mitochondrial calcium uptake and energetic mismatch in a rat model of takotsubo cardiomyopathy

N. Godsman[1]; M. Kohlhaas[2]; A. Nickel[2]; L. Cheyne[1]; D. Dawson[1]; C. Maack[2]
[1]University of Aberdeen, Aberdeen, United Kingdom; [2]Comprehensive Heart Failure Center (CHFC), Wurzburg, Germany

Background: Takotsubo cardiomyopathy (TTC) is an acute heart failure syndrome with a typical left ventricular "ballooning" and in-hospital mortality rates of 4-5%. Human studies revealed severe energetic impairment during the acute phase of this condition.

Purpose: The mechanisms of such energetic impairment, however, are unresolved. Here, we characterise mitochondrial function in an animal model of TTC.

Methods: The TTC model was induced by intraperitoneal injection of isoprenaline (100 mg/kg) in 2-4 months old female Sprague Dawley rats (254 ± 25 g). Our previous studies revealed a TTC-like apical ballooning of the left ventricle at day 3 after injection, which resolved at day 7. Accordingly, cardiac myocytes and mitochondria were isolated at 3 and 7 days post-injection from TTC and control hearts (n=7, respectively). Cardiac myocytes were field stimulated and submitted to a physiological stress protocol (5 Hz stimulation plus β-adrenergic stimulation) during which the redox states of NAD(P)H and FAD (autofluorescence), cytosolic [Ca2+] (Indo-1) and mitochondrial membrane potential (TMRM) were determined together with sarcomere length. In a parallel set of experiments, cytosolic and mitochondrial [Ca2+] were determined in a fluorescence- (rhod-2/Indo-1) and patch-clamp-based approach. In isolated mitochondria, O2 consumption (Clark electrode), reactive oxygen species (ROS) emission (Amplex red) and Ca2+ uptake (Ca2+ green assay) were assessed.

Results: At 3 and 7 days after injection, basal respiration, Ca2+ uptake and ROS emission were similar in isolated mitochondria from TTC and control hearts. In isolated cardiac myocytes at day 3, systolic and diastolic cytosolic [Ca2+] were slightly reduced in TTC vs control hearts during maximal β-adrenergic stimulation (p<0.05), while sarcomere length and systolic shortening were unchanged. In patch-clamp experiments (with the cytosol being equilibrated by pipette solution), mitochondrial Ca2+ uptake was impaired despite increased cytosolic Ca2+ transients at day 3 in TTC cells. Accordingly, the redox states of mitochondrial NAD(P)H and FAD were moderately, but significantly oxidised during workload transitions at day 3, reflecting impaired Ca2+-induced stimulation of the Krebs cycle in TTC. These defects in mitochondrial Ca2+ uptake and redox adaptations were resolved at day 7.

Conclusions: Defects in mitochondrial Ca2+ uptake provoke energy supply-and-demand mismatch which may account for energetic deficit and oxidative stress in TTC, while mitochondria appear to maintain a level of functional integrity in isolation. Further research will therefore address the detailed mechanisms of impaired mitochondrial Ca2+ uptake and whether therapeutic interventions to ameliorate these defects influence the phenotype of TTC.

P137

Cardiomyopathy-associated arginine-mutations within the RS-domain of RBM20 lead to mislocalization of the protein

A. Gaertner-Rommel[1]; J. Bloebaum[1]; B. Klauke[1]; U. Schulz[2]; J. Gummert[2]; H. Milting[1]
[1]Heart and Diabetes Center NRW, Erich und Hanna Klessmann-Institut für Kardiovaskuläre Forschung und Entwicklung, Bad Oeynhausen, Germany; [2]Heart and Diabetes Center NRW, Bad Oeynhausen, Germany

Introduction: Mutations in human RBM20 have previously been shown to cause dilated cardiomyopathy (DCM). Within the nucleus RBM20 partially colocalises with other splice factors, binds RNA and has a major role in myocardial alternative splicing.

We have identified in our patient cohort the previously published RBM20 mutation p.P638L and two novel mutations, p.S635C and p.S635F, which are localized in the highly conserved RS-domain. The mutations are highly penetrant leading to terminal heart failure and/or to sudden cardiac death. Previous studies from our laboratory showed subcellular mislocalisation of these mutant RBM20-proteins presumably due to aberrant phosphorylation. Though cardiomyopathy-associated mutations affecting arginines within the conserved RS-domain are known from the literature, little is known on the molecular pathomechanisms of these mutations.

Purpose: Goal of this study was to gain further insight into mutation-associated mislocalisation of RBM20 by analyzing the effects of arginine-mutations within the conserved RS-domain on the intracellular distribution of RBM20. Furthermore, we proved if the position of the affected serine within the RS-domain has an effect on nuclear localization.

Methods: To compare the localization of RBM20 wildtype and mutants we constructed RBM20-EYFP protein chimera and analyzed their subcellular localization in different cell lines. To estimate the influence of phosphorylation we analyzed the localization of phosphomimetic mutants of RBM20. We analyzed the cellular localization of protein mutants related to the arginines on positions 632, 634, 636 and 641 and the serines at positions 635, 637 and 640 of RBM20.

Results: Comparable to serine mutations, mutations concerning the highly conserved arginines within the RS-domain also lead to a subcellular mislocalization of RBM20. Interestingly, the kind and position of amino acid exchange seems to be important for the extent of nuclear misdistribution. Comparing the intracellular localization of serine non-phosphomimetic and phosphomimetic mutants we could show that in contrast to serines at positions 635 and 637 the exchange of the serine at position 640 does not lead to a complete loss of nuclear localization of RBM20.

Conclusions: We present here first data showing that mutations affecting the conserved arginines within the RS-domain of RBM20 lead to a subcellular mislocalisation of the protein likely leading to aberrant splicing. Furthermore, our results indicate that the highly conserved amino acids within the RS-domain play different roles in nuclear transport and/or retention of RBM20.